

Cite this: *Chem. Sci.*, 2021, **12**, 10732

All publication charges for this article have been paid for by the Royal Society of Chemistry

Received 9th May 2021  
Accepted 14th June 2021

DOI: 10.1039/d1sc02551a  
[rsc.li/chemical-science](http://rsc.li/chemical-science)

## Non-metal with metal behavior: metal-free coordination-insertion ring-opening polymerization†

Xin Wang, <sup>ac</sup> Jiaxi Xu, <sup>ac</sup> Zhenjiang Li, <sup>a</sup> Jingjing Liu, <sup>ac</sup> Jie Sun, <sup>b</sup> Nikos Hadjichristidis, <sup>\*c</sup> and Kai Guo, <sup>\*a</sup>

The “coordination-insertion” ring-opening polymerization (ROP) mechanism has so far been the monopoly of metal catalysts. In this work, we present a metal-free “coordination-insertion” ROP of trimethylene carbonate (TMC) and  $\varepsilon$ -caprolactone ( $\varepsilon$ -CL), as well as their sequential block copolymerization, with *N*-trimethylsilyl-bis(trifluoromethanesulfonyl)imide (TMSNTf<sub>2</sub>) as the non-metallic initiator/catalyst. TMSNTf<sub>2</sub> was proposed to work through an unprecedented metal-free “coordination-insertion” mechanism, which involves the coordination of monomer to the Si atom of TMSNTf<sub>2</sub>, the nucleophilic attack of the  $-NTf_2$  group on the coordinated monomer, and the cleavage of the acyl–oxygen bond of the monomer. The proposed metal-free “coordination-insertion” ROP was studied by NMR, SEC, and MALDI-TOF analyses. In addition, the TMSNTf<sub>2</sub>-mediated ROP of TMC and  $\varepsilon$ -CL led to linear and cyclic polymers following two-stage first-order polymerization processes, as evidenced by structural analyses and kinetics study, which further demonstrated the metal-free “coordination-insertion” mechanism.

## Introduction

A primary axiom of the definition of Lewis acid-base is the notion that the combination of a simple Lewis acid and Lewis base results in the neutralization reaction to form “classical” Lewis acid/Lewis base adducts.<sup>1</sup> An exception is the transition metal-ligand complex,<sup>2</sup> which is a single molecule that contains both Lewis acid and Lewis base activation sites and can simultaneously carry out both electrophilic and nucleophilic activation in chemical reactions (Scheme 1). The most representative example is the transition metal alkoxides,<sup>2d,3</sup> which possess metal Lewis acid centers with vacant orbitals and Lewis base ligands with lone pair electrons. The metal alkoxides can initiate/catalyze the ring-opening polymerization (ROP) of cyclic esters through a “coordination-insertion” mechanism, which has been extensively used in the aliphatic polyesters industrial production. However, so far, the metal-free “coordination-insertion” ROP has not been reported.

Numerous recent discoveries have shown that several non-metallic main group elements behave like metals (metalloid).<sup>4</sup> The non-metallic elements possess open/stable low-valent derivatives with either open<sup>5</sup> or quasi-open coordination sites.<sup>6</sup> Among the metalloid elements, silicon (the second richest element on earth, only after oxygen) is a suitable candidate, since it can expand its coordination sphere and reach a “hypervalent” state and thus giving rise to five- and six-coordinate intermediates. The reported various Lewis base donor-stabilized Si compounds demonstrate the unsaturated coordination character of the silicon atom.<sup>7</sup> At present, we selected a silicon–nitrogen compound [*N*-trimethylsilyl-bis(trifluoromethanesulfonyl)imide (TMSNTf<sub>2</sub>)] to test the possibility of metal-free “coordination-insertion” ROP. The selected silicon–nitrogen compound has a lone pair electron center (tertiary amine) and vacant orbitals (Si atom), similar to metal alkoxide compounds, as shown in Scheme 1. In the case of metal-alkoxides, the “coordination-insertion” mechanism involves the coordination of the monomer with the metal Lewis-acid center, and the insertion of the monomer into the metal-alkoxide bond *via* the nucleophilic addition of Lewis base ligands (Scheme 1). Therefore, the silicon–nitrogen compound is a promising candidate to promote metal-free “coordination-insertion” in ROP.

In this work, trimethylene carbonate (TMC) was chosen as a model monomer to perform the ROP with TMSNTf<sub>2</sub> to verify the metal-free “coordination-insertion” mechanism (Scheme 2). The synthesis of TMSNTf<sub>2</sub> was achieved by reaction of bis(trifluoromethanesulfonyl)imide (HNTf<sub>2</sub>) with

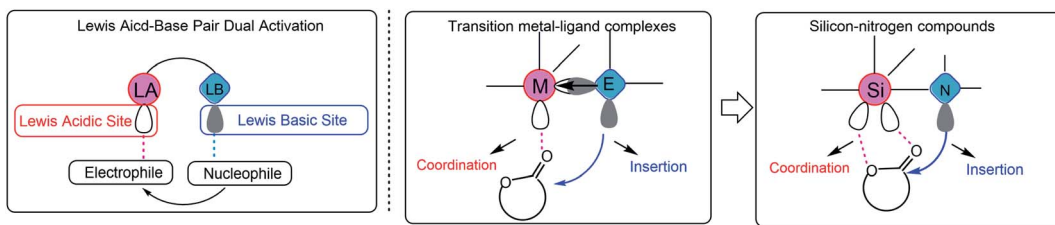
<sup>a</sup>State Key Laboratory of Materials-Oriented Chemical Engineering, College of Biotechnology and Pharmaceutical Engineering, Nanjing Tech University, 30 Puzhu Road South, Nanjing 211816, China. E-mail: guok@njtech.edu.cn

<sup>b</sup>College of Food Science and Light Industry, Nanjing Tech University, 30 Puzhu Road South, Nanjing 211816, China

<sup>c</sup>Physical Sciences and Engineering Division, KAUST Catalysis Center, Polymer Synthesis Laboratory, King Abdullah University of Science and Technology (KAUST), Thuwal 23955, Saudi Arabia. E-mail: nikolaos.hadjichristidis@kaust.edu.sa

† Electronic supplementary information (ESI) available. See DOI: 10.1039/d1sc02551a





**Scheme 1** Possible “coordination-insertion” mechanism in ROP of cyclic esters by silicon–nitrogen compound, inspired by the transition metal–ligand complexes.

allyltrimethylsilane.<sup>8</sup> However, if  $\text{HNTf}_2$  is not consumed completely, the residual  $\text{HNTf}_2$  interferes, since it also polymerizes TMC by a cationic mechanism leading to polycarbonates with ether units (decarboxylation) as detected by nuclear magnetic resonance (NMR) spectroscopy.<sup>9</sup> The absence of the ether units excludes the presence of  $\text{HNTf}_2$ . In contrast,  $\text{TMSNTf}_2$  initiates/catalyzes the ROP of TMC while preventing undesirable decarboxylation reactions. Besides, the ROP of  $\epsilon$ -caprolactone and the block ring-opening sequential copolymerization of  $\epsilon$ -CL and TMC were studied with  $\text{TMSNTf}_2$  as initiator/catalyst. To shed light on the polymerization mechanism, we studied: (a) the kinetics of ROP by NMR and size-exclusion chromatography (SEC), (b) the structure of the products by NMR and matrix-assisted laser desorption/ionization-time of flight (MALDI-TOF) mass spectrometry, (c) the structure of the growing chain, and (d) the monomer activation by  $\text{TMSNTf}_2$  with NMR titration experiments.

## Results and discussion

### Ring-opening polymerization

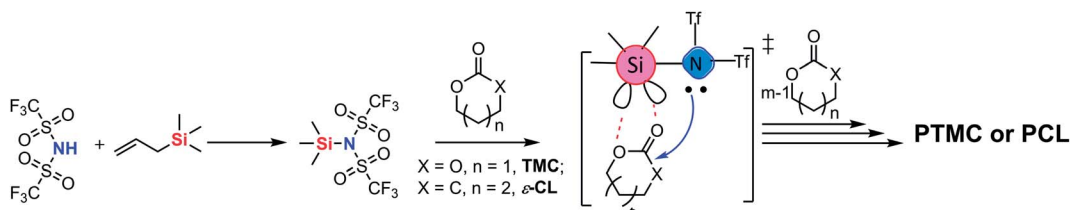
Initially, to exclude the possibility that the super-strong Brønsted acid  $\text{HNTf}_2$  promotes the ROP, we investigated the catalytic performance of  $\text{HNTf}_2$  in the ROP of TMC (Table 1, entry 1). As anticipated,  $\text{HNTf}_2$  showed weak control over TMC polymerization with apparent decarboxylation. Due to the extremely strong Brønsted acidity of  $\text{HNTf}_2$ , the undesirable elimination of carbon dioxide during the polymerization seemed to be unavoidable under room temperature. From the  $^1\text{H}$  NMR spectrum, the ether unit was determined by the triplet signal at 3.47 ppm attributed to methylene protons next to ether oxygen, as shown in Fig. S1.<sup>†</sup>

Surprisingly, the ROP of TMC by the *in situ* generating  $\text{TMSNTf}_2$  reached 95% in 10 h when the acidity of  $\text{HNTf}_2$  was regulated by allyltrimethylsilane (ATMS), and TMC was

completely converted to poly(trimethylene carbonate) (PTMC) without any decarboxylation (Table 1, entry 2). The chemical structure of PTMC was confirmed by NMR (Fig. 1). There is no triplet signal of polyether at 3.47 ppm (Fig. 1a), which suggests that the  $\text{TMSNTf}_2$ -mediated polymerization proceeded homogeneously without the elimination of  $\text{CO}_2$ . Also, the peaks of the polymer main chain appeared at 2.04 and 4.20–4.24 ppm, the methylene protons adjacent to the  $\omega$ -chain end of the hydroxyl group appeared at 3.73 ppm. In addition, the  $^{13}\text{C}$  NMR spectrum (Fig. 1b) shows all the characteristic signals of the PTMC, thus further confirming that the  $\text{TMSNTf}_2$ -mediated polymerization of TMC proceeds without decarboxylation with complete conversion of  $\text{HNTf}_2$  to  $\text{TMSNTf}_2$ .  $\text{TMSNTf}_2$ -mediated ROP of  $\epsilon$ -CL was also carried out with  $[\epsilon\text{-CL}]_0/[\text{TMSNTf}_2]_0 = 20/1$  (Table 1, entry 6). The conversion of monomer reached 98.1% in 9 h. From the NMR analysis (Fig. S2<sup>†</sup>), the chemical structure of PCL was confirmed, revealing that the  $\text{TMSNTf}_2$  successfully mediated the ROP of  $\epsilon$ -CL. Taking into account all the above results, we conclude that only  $\text{TMSNTf}_2$  and no residual  $\text{HNTf}_2$  are involved in the metal-free ROP of both cyclic carbonate and lactone monomers.

### Mechanism

To obtain an insight into the  $\text{TMSNTf}_2$ -mediated ROP mechanism, we determined the end-chain structure of the synthesized PTMC and PCL by MALDI-TOF MS. In the MALDI-TOF mass spectra of PTMC (Fig. 2), three series of molecular ion peaks are present, a major linear PTMCs with hydroxyl end group (HO-PTMC-H), and two minors, one of which is cyclic (C-PTMC-C) and the other one linear PTMCs with methoxyl end group (MeO-PTMC-H). In the MALDI-TOF spectra of PCL (Fig. S4<sup>†</sup>), two series of molecular ion peaks appear, a major which is consistent with linear PCLs having hydroxyl end groups (HO-PCL-H) and a minor corresponding cyclic PCLs (C-PCL-C). The



**Scheme 2** ROP of TMC and  $\epsilon$ -CL by the *in situ* generated  $\text{TMSNTf}_2$ .



Table 1  $\text{HNTf}_2$  and  $\text{TMSNTf}_2$  initiated/catalyzed ROP of TMC and  $\varepsilon\text{-CL}$  in  $\text{CH}_2\text{Cl}_2$ <sup>a</sup>

Entry	Monomer	Catalyst and initiator	$[\text{M}]_0/[\text{I}]_0$	Time/h	Conv. %	$M_n$ (theor) <sup>d</sup>	$/\text{kg mol}^{-1}$	$M_n$ (NMR) <sup>e</sup>	$/\text{kg mol}^{-1}$	$M_n$ (SEC) <sup>f</sup>	$/\text{kg mol}^{-1}$	$D^f (M_w/M_n)$
1	TMC	$\text{HNTf}_2 + \text{BnOH}^b$	20/1	3	96	1.9		n.d.		1.0		1.29
2	TMC	$\text{TMSNTf}_2$	20/1	10	95	1.9		2.1		3.6		1.22
3	TMC	$\text{TMSNTf}_2$	50/1	15	97	5.0		5.4		6.1		1.17
4	TMC	$\text{TMSNTf}_2$	70/1	18	95	6.8		6.6		7.2		1.10
5	TMC	$\text{TMSNTf}_2$	100/1	24	94	9.6		9.7		9.0		1.12
6	$\varepsilon\text{-CL}$	$\text{TMSNTf}_2$	20/1	9	98	2.2		2.9		4.0		1.25
7	$\varepsilon\text{-CL}$	$\text{TMSNTf}_2$	30/1	14	98	3.3		4.1		5.8		1.22
8	$\varepsilon\text{-CL}$	$\text{TMSNTf}_2$	50/1	21	95	5.4		5.8		6.5		1.18
9	$\varepsilon\text{-CL}$	$\text{TMSNTf}_2$	70/1	26	96	7.6		7.3		7.4		1.09
10	$\varepsilon\text{-CL}$	$\text{TMSNTf}_2$	100/1	32	93	10.6		9.8		9.2		1.15
11	$\delta\text{-VL}$	$\text{TMSNTf}_2$	50/1	13	91	4.8		4.7		5.4 <sup>g</sup>		1.21 <sup>g</sup>
12	L-LA	$\text{TMSNTf}_2$	50/1	48	0	n.d.		n.d.		n.d.		n.d.

<sup>a</sup> Room temperature,  $[\text{TMC}]_0 = 0.7 \text{ mol L}^{-1}$ ,  $[\varepsilon\text{-CL}]_0 = 1.0 \text{ mol L}^{-1}$ . <sup>b</sup>  $[\text{HNTf}_2]_0/[\text{BnOH}]_0 = 1/1$ . <sup>c</sup> Determined by  $^1\text{H}$  NMR in  $\text{CDCl}_3$  using integrals of the characteristic signals. <sup>d</sup> Theoretical molecular weights were calculated based on conversion and the  $[\text{M}]_0 : [\text{I}]_0$  ratio. <sup>e</sup> Determined by  $^1\text{H}$  NMR in  $\text{CDCl}_3$  by comparing the integration area of the chain end methylene group with that of the corresponding methylene at the repeating units. <sup>f</sup> Determined by a tandem SEC-MALS-DRI system using the  $dn/dc$  [ $0.0409 \text{ mL g}^{-1}$ ] of PTMC and  $dn/dc$  [ $0.070 \text{ mL g}^{-1}$ ] of PCL in THF at room temperature. <sup>g</sup> Determined by SEC in THF using PSt standards.

mass difference between the neighboring peaks corresponds to the  $\varepsilon\text{-CL}$  monomeric unit of  $m/z = 114.07$ . However, the already reported mechanisms for another silicon Lewis acid-initiated ROP of cyclic carbonates and lactones could not explain our results.<sup>10</sup> In the case of TMC, the silicon Lewis acid can participate in two pathways (Fig. S3†): in the first one, the monomer carbonyl oxygen attacks its cationic silicon site (“cationic mechanism”), and in the second one, it functions as a ligand coordinating with the carbonyl oxygen *via* the vacant d orbitals.

Nevertheless, according to both reported mechanisms, it will be impossible to achieve controlled TMC polymerization without ether units in the backbone, since the formed silicon ester (Fig. S3†) leads to an inevitable decarboxylation and generation of silyl ether unit ( $m/z = 58.04$ ).<sup>10</sup> In our MALDI-TOF spectra of PTMC, the mass differences between the neighboring peaks of each series of molecular ion peaks were identical to the molecular weight of the TMC monomeric unit ( $m/z = 102.03$ ). Such results exclude the “cationic mechanism” promoted by  $\text{HNTf}_2$ .

Inspired by the coordination-insertion mechanism of the metallic complexes initiated/catalyzed ROP of cyclic esters,<sup>2d,11</sup> we propose a metal-free “coordination-insertion” mechanism of  $\text{TMSNTf}_2$  for the ROP of cyclic carbonates and lactones. Based on the extension of the donor–acceptor concept proposed by Viktor Gutmann,<sup>12</sup> in a molecule with the intramolecular donor–acceptor interaction, the interaction will lead to the enhanced polarity and electrophilicity of the acceptor atom and the enhanced nucleophilicity property of the donor atom. The longer bond between the acceptor atom and the donor atom, the greater the electrophilicity and the nucleophilicity of the corresponding atom will be. In our case,  $\text{TMSNTf}_2$  has the intramolecular donor–acceptor interaction, N is the electron donor, Si is the electron acceptor, and the N–Si of  $\text{TMSNTf}_2$  is a relatively long bond.<sup>13</sup> Therefore, both the enhanced nucleophilicity of the tertiary amine and the enhanced electrophilicity of the silicon group in  $\text{TMSNTf}_2$  can take place. When  $\text{TMSNTf}_2$  is used as initiator/catalyst in ROP, the Si-group may act as

a coordination center and the  $-\text{NTf}_2$  as a unique nucleophile. In a coordination-insertion mechanism, besides the formation of the expected linear polymer, chain termination frequently occurs *via* intramolecular back-biting reactions to yield a cyclic polymer,<sup>14</sup> which explains the existence of cyclic PTMC and PCL in our MALDI-TOF MS spectra. Besides, we even speculate that  $-\text{SiMe}_3$  is attached to the O-end forming  $(\text{Me})_3\text{Si-polymer-NTf}_2$  with weak interaction. Then upon methanolysis or hydrolysis,<sup>15</sup> the Si-alkoxide group is transformed into hydroxyl end-group. Moreover, due to the easy leaving character of  $-\text{NTf}_2$ ,<sup>16</sup>  $\text{H}_2\text{O}$  or alcohols can react (nucleophilic attack) with the carbonyl- $\text{NTf}_2$  to generate polymers with alkoxy end-group. Based on the metal-free “coordination-insertion” mechanism, it is reasonable to explain the existence of several series of molecular ion peaks corresponding to linear polymers and cyclic polymers in the MALDI-TOF spectra of PTMC and PCL.

As suggested by the MALDI-TOF spectra of PTMC (Fig. 2), peaks corresponding to linear PTMCs (HO-PTMC-H) are the most intensive ones, following by the linear PTMCs (MeO-PTMC-H) and the cyclic PTMCs (C-PTMC-C). The formation of MeO-PTMC-H and HO-PTMC-H may be due to the water coming from the air. The water enters the mixture when the reaction tube is opened to the air after the polymerization is completed. Consequently, the water attacks the carbonyl- $\text{NTf}_2$  of PTMC before the addition of methanol, leading to hydrolysis/CO<sub>2</sub> release and thus producing the major linear HO-PTMC-H component. From the MALDI-TOF spectra of PCL (Fig. S4†), only a major family of linear PCL with hydroxyl end group (HO-PCL-H) and a minor one of cyclic PCL (C-PCL-C) are apparent. The carbonyl- $\text{NTf}_2$  connection in  $(\text{Me})_3\text{Si-PCL-NTf}_2$  is more stable than the ester- $\text{NTf}_2$  one in  $(\text{Me})_3\text{Si-PTMC-NTf}_2$ , and therefore, the methanol cannot replace  $-\text{NTf}_2$  in  $(\text{Me})_3\text{Si-PCL-NTf}_2$  in the very short precipitation time. But the hydrolysis of the obtained polymer by the inevitable moisture in the air occurs in a relatively long storage time after precipitation. Therefore, only HO-PCL-H appears in the MALDI-TOF spectra of PCL. Besides, the intramolecular back-biting reactions are



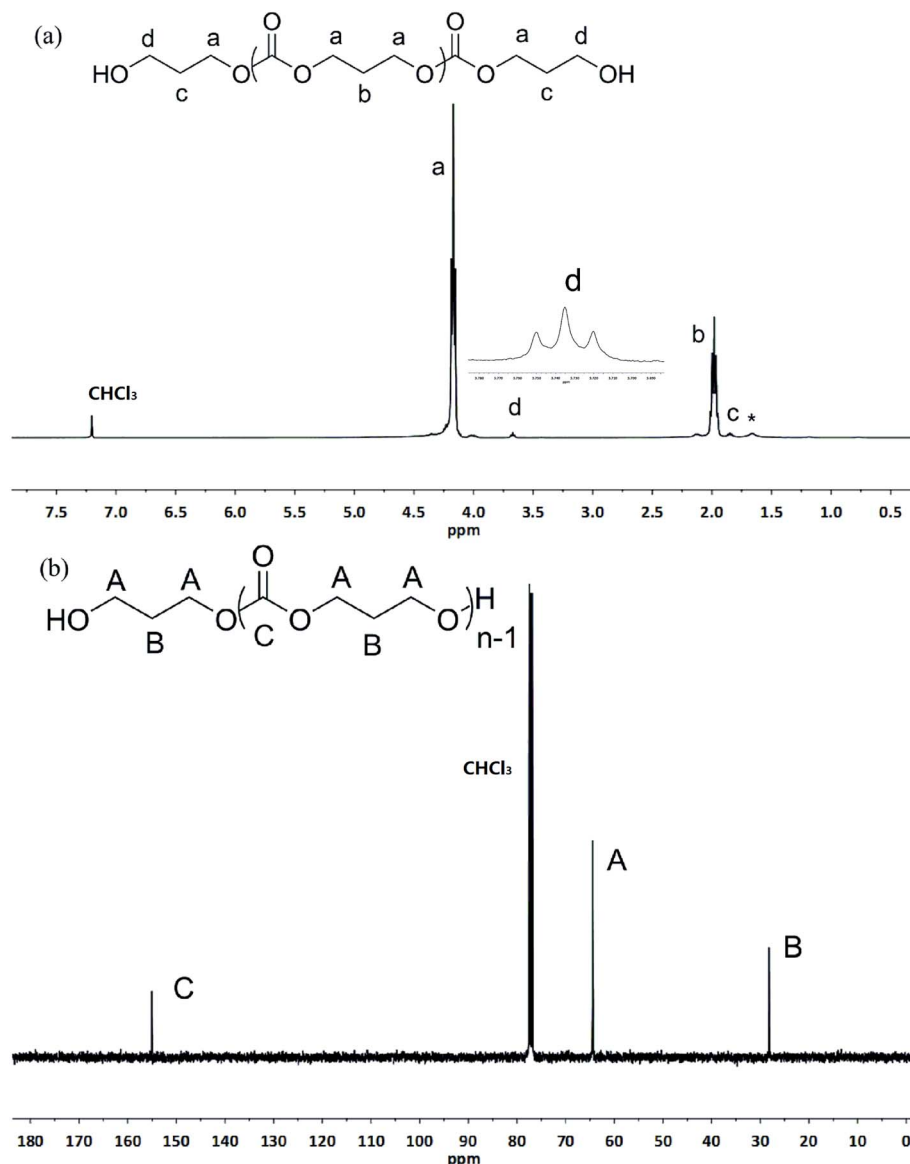


Fig. 1  $^1\text{H}$  NMR (a) and  $^{13}\text{C}$  NMR (b) spectra of the obtained PTMC ( $[\text{M}]_0/[\text{I}]_0 = 20$ , Table 1, entry 2) initiated by  $\text{TMSTf}_2$  (asterisk refers to the residual water in polymers).

inevitable in the “coordination-insertion” polymerization, the reason that in the MALDI-TOF spectra of both PTMC and PCL, cyclic structures are present even though in very low content.

Since the water coming from the air enters the polymerization mixture, which leads to linear polymers with hydroxyl end group (major family), we then investigated the polymers produced by  $\text{TMSTf}_2$ -mediated ROP of TMC and  $\varepsilon$ -CL, without quenching, and precipitated by super dry methanol in the glovebox. In the MALDI-TOF mass spectra (Fig. 3A) of the PTMC, the peaks of PTMCs shifted from the predominantly linear PTMCs with hydroxyl end group to the mostly linear PTMCs with methoxyl end group instead. As we assumed, the MALDI-TOF spectra consist of two series of molecular ion peaks, with the major series (A, a) assigning to the linear PTMCs (MeO-PTMC-H) and the minor series (B, b) to the cyclic PTMCs.

Furthermore, the structure of the linear PTMC (MeO-PTMC-H) was also confirmed by  $^1\text{H}$  and  $^{13}\text{C}$  NMR (Fig. S5†), as evidenced by the resonance at  $\delta$  3.77 ( $\text{CH}_3\text{OCOO}^-$ ) in  $^1\text{H}$  NMR spectrum and the resonance at  $\delta$  51.1 ( $\text{CH}_3\text{OCOO}^-$ ) in the  $^{13}\text{C}$  NMR spectrum. These results indicate that methanol behaves as a nucleophile to attack the carbonyl- $\text{NTf}_2$  of PTMC during the precipitation procedure when  $\text{H}_2\text{O}$  was excluded.

As shown in Fig. 3B, the series of molecular ion peaks of  $\text{Tf}_2\text{N-PCL-H}$  appear clearly in the MALDI-TOF MS spectra of PCL, which directly evidenced that the  $-\text{NTf}_2$  nucleophilically attacks the carbonyl carbon of monomer in the initiation step of the ring-opening process. Further confirmation is provided by the  $^{13}\text{C}$  NMR and  $^{19}\text{F}$  NMR, as evidenced by the resonance at  $\delta$  124.8–128.7 ( $(\text{CF}_3\text{SO}_2)_2\text{N}^-$ ) in the  $^{13}\text{C}$  NMR spectrum (Fig. S6†) and the resonance at  $\delta$  –72.02 ( $(\text{CF}_3\text{SO}_2)_2\text{N}^-$ ) in the  $^{19}\text{F}$  NMR

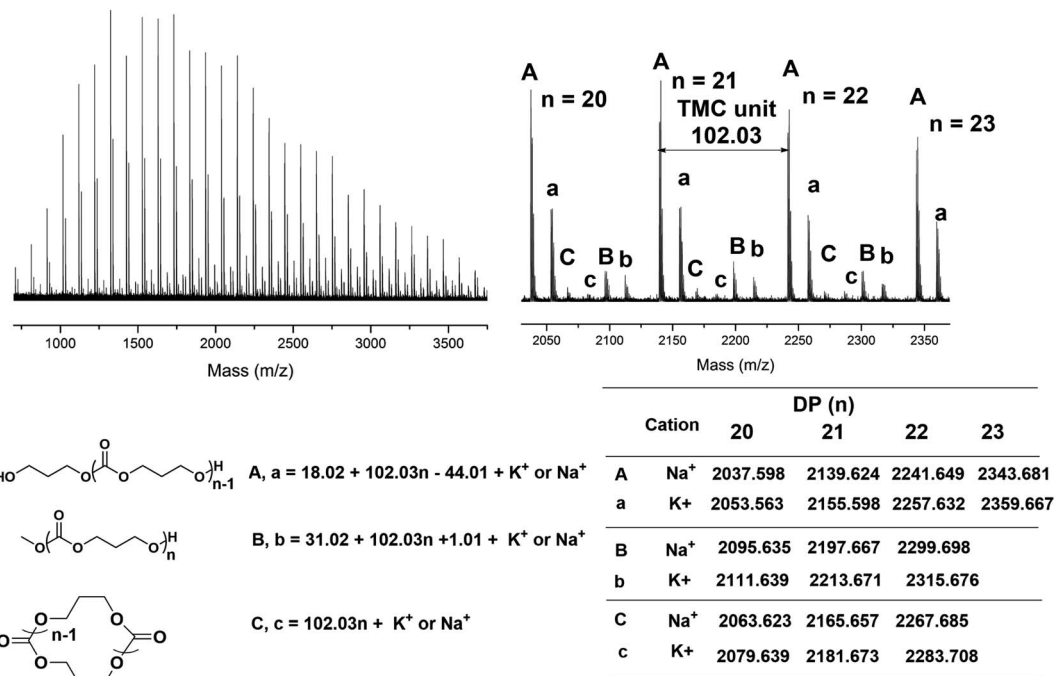


Fig. 2 MALDI-TOF MS spectra of the obtained PTMC ( $[\text{M}]_0/[\text{I}]_0 = 20$ , Table 1, entry 2) initiated by  $\text{TMSNTf}_2$ .

spectrum (Fig. S7†). In contrast,  $\text{Tf}_2\text{N-PTMC-H}$  could never be captured by both MALDI-TOF MS and NMR measurements, which verifies the more stability of the  $\text{Tf}_2\text{N-CO-}$  in  $\text{Tf}_2\text{N-PCL-H}$  than that of  $\text{Tf}_2\text{N-OCO-}$  in  $\text{Tf}_2\text{N-PTMC-H}$ . Additionally, major HO-PCL-H still appears, but MeO-PCL-H is not present in the MALDI-TOF MS spectra of PCL (Fig. 3B). These results confirmed that the methanol cannot break the ester- $\text{NTf}_2$  connection of  $(\text{Me})_3\text{Si-PTMC-NTf}_2$  in a very short precipitation time. The major HO-PCL-H also comes from the hydrolysis of  $\text{Tf}_2\text{N-PCL-H}$  by the inevitable moisture in the air after precipitation. Besides, in the MALDI-TOF MS spectra of PTMC (Fig. 2 and 3) and PCL (Fig. S4† and 3), the presence of small amount of cyclic polymers proves that the intramolecular back-biting reactions<sup>17</sup> are not dominant during the  $\text{TMSNTf}_2$ -mediated

ROP. Similar phenomena were also observed in other metal-complex initiated ring-opening polymerization.<sup>18</sup>

Since nucleophiles (methanol and water) can replace the  $\text{Tf}_2\text{N-}$  end group of PCL, benzyl alcohol and 2,2-diphenylethanol were also carried out to replace the  $\text{Tf}_2\text{N-}$  end group of PCL. Excess benzyl alcohol or 2,2-diphenylethanol was added at the end of the polymerization of  $\varepsilon\text{-CL}$  ( $[\varepsilon\text{-CL}]_0/[\text{TMSNTf}_2]_0 = 20/1$ ). The reaction was then kept 4 h at room temperature under stirring. Then PCL was obtained from precipitation in methanol three times and drying by vacuum oven for 24 h. The  $^1\text{H}$  NMR spectra (Fig. S8†) proved that benzyl alcohol or 2,2-diphenylethanol successfully replaced the end group  $-\text{NTf}_2$  in PCL. Therefore, the easily replaceable  $-\text{NTf}_2$  provides a method for post-modification of polymer end groups.

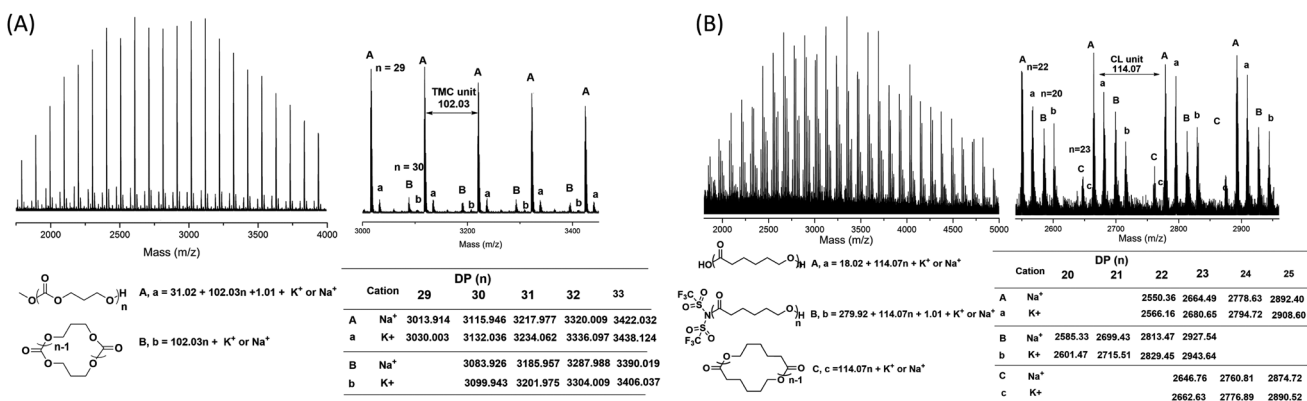


Fig. 3 MALDI-TOF MS spectra of (A) PTMC ( $[\text{M}]_0/[\text{I}]_0 = 20$ ) and (B) PCL ( $[\text{M}]_0/[\text{I}]_0 = 20$ ) initiated by  $\text{TMSNTf}_2$ , without quenching, and precipitated by super dry methanol in the glovebox.

In addition, the  $\text{TMSNTf}_2$  mediated-ROP of  $\delta$ -VL ( $[\text{TMSNTf}_2]_0/[\delta\text{-VL}]_0 = 1/50$ ) was carried out (Table 1, entry 11). The conversion of monomer reached 90.6% in 13 h. The polymer was also obtained from the precipitation in super dry methanol. The structure of PCL with the methoxy end group was confirmed by  $^1\text{H}$  NMR (Fig. S10 $\dagger$ ). According to the MALDI-TOF mass spectra (Fig. S11 $\dagger$ ) of the obtained PVL, the series of molecular ion peaks of  $\text{Tf}_2\text{N-PVL-H}$  appear clearly. Furthermore, the existence of  $-\text{NTf}_2$  at the end of the polymer was further evidenced by  $^{19}\text{F}$  NMR with the resonance at  $\delta = -72.00$  ppm ( $(\text{CF}_3\text{SO}_2)_2\text{N}^-$ ) in the  $^{19}\text{F}$  NMR spectrum (Fig. S12 $\dagger$ ). The  $-\text{NTf}_2$  nucleophilically attacks the carbonyl carbon of monomer in the initiation step of the ring-opening process was again confirmed in the  $\text{TMSNTf}_2$  mediated-ROP. We also carried out the  $\text{TMSNTf}_2$  mediated-ROP of L-lactide (Table 1, entry 12). Unfortunately, no polymer was obtained after 48 h, since the first attempt of metal-free “coordination-insertion” catalyst does not have strong enough activation to the carbonyl group of lactide in ROP. Above all, the nucleophilic capacity of the  $-\text{NTf}_2$  group in  $\text{TMSNTf}_2$  was proved.

To explain the coordination of Si atom in  $\text{TMSNTf}_2$  with the monomer, the interaction between  $\text{TMSNTf}_2$  and monomer was studied by NMR. Unfortunately, when  $\text{TMSNTf}_2$  was titrated with TMC or  $\epsilon$ -CL, the adduct monomer/ $\text{TMSNTf}_2$  was difficult to observe since propagation occurred immediately. An excellent alternative monomer to study the interaction at initiation is  $\gamma$ -butyrolactone ( $\gamma$ -BL) since it has a positive enthalpy of polymerization and does not polymerize at room temperature.<sup>2b</sup> When  $\text{TMSNTf}_2$  (0.25 equiv.) was titrated with  $\gamma$ -BL (1 equiv.), the  $^{13}\text{C}$  chemical shift of the carbonyl carbon ( $\gamma$ -BL) moved downfield from 177.83 ppm to 178.62 ppm (Fig. 4), due to its coordination with the Si of  $\text{TMSNTf}_2$  (deshielding). When  $\text{TMSNTf}_2$  was increased (0.5–2 equiv.), keeping the same  $\gamma$ -BL (1 equiv.), their chemical shifts moved downfield constantly. Furthermore, methylene carbon adjacent to ester oxygen was moved downfield with the increasing molar ratios of  $\text{TMSNTf}_2$  to  $\gamma$ -BL (Fig. 4). These results suggest that Si atom coordinates to ester oxygen, and therefore, the electronic density is depressed, rendering the methylene carbon also deshielded. In

addition, the mixture of  $\text{TMSNTf}_2$  (1.0 equiv.) and  $\gamma$ -BL (1.0 equiv.) was studied by  $^{29}\text{Si}$  NMR. As shown in Fig. S13, $\dagger$  when  $\text{TMSNTf}_2$  was titrated with  $\gamma$ -BL, the  $^{29}\text{Si}$  chemical shift of  $\text{TMSNTf}_2$  moved to highfield relative to pure  $\text{TMSNTf}_2$ . This is because the electron density of silicon atom is enhanced (shielding) through the coordination to the oxygen of  $\gamma$ -BL. All these data indicate that  $\text{TMSNTf}_2$  activates the monomer by coordination with both carbonyl oxygen and ester oxygen.

Based on the above results, we proposed the first metal-free “coordination-insertion” mechanism of  $\text{TMSNTf}_2$ -mediated ROP of cyclic carbonates and lactones presented in Scheme 3, for TMC as a model monomer. The Si atom carries four  $\text{sp}^3$  orbitals and five empty electron-accepting d orbitals, similar to Sn atom, used in the metallic coordination-insertion mechanism.<sup>4</sup> Two of the vacant orbitals coordinate with the carbonyl and ester oxygen of the TMC, simultaneously, followed by a nucleophilic attack of  $-\text{NTf}_2$  on the carbonyl carbon and acyl-oxygen cleavage to form a silicon-alkoxo active end group. This initiation step is followed by continuous TMC insertion into the silicon-alkoxo bond. During the polymerization, a small amount of intramolecular transesterification occurs leading to the formation of cyclic structures. When the monomer is totally consumed, the polymer is precipitated in methanol. The nucleophile  $\text{MeOH}$  or  $\text{H}_2\text{O}$  attacks the carbonyl carbon connected to  $-\text{NTf}_2$  leading to the elimination of  $-\text{NTf}_2$  end-group. Both initiation and propagation follow the pattern of the “coordination-insertion” mechanism, which in the past was exclusively the monopoly of metal complexes.

Below additional evidence is provided to support our proposed metal-free “coordination-insertion” ROP-mediated by  $\text{TMSNTf}_2$ . The ROP of TMC/ $\text{TMSNTf}_2$  in a ratio of 10 : 1 before quenching was studied by  $^{13}\text{C}$  NMR conducted in Teflon-valve-sealed J. Young-type NMR tubes, which fully excluded the influence of  $\text{H}_2\text{O}$  and other nucleophiles. The presence of the end group corresponding to  $-\text{CH}_2\text{CH}_2\text{CH}_2\text{O-Si}(\text{CH}_3)_3$  was detected, as shown in Fig. S14. $\dagger$  Moreover, in Teflon-valve-sealed J. Young-type NMR tubes,  $\epsilon$ -CL/ $\text{TMSNTf}_2$  in a ratio of 1 : 1 without quenching was also studied by  $^{13}\text{C}$  NMR. As shown in Fig. S15b, $\dagger$  the end group corresponding to

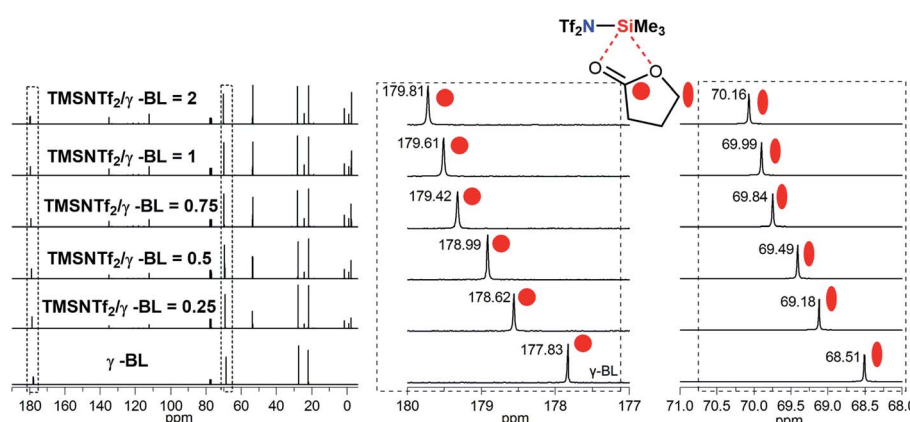
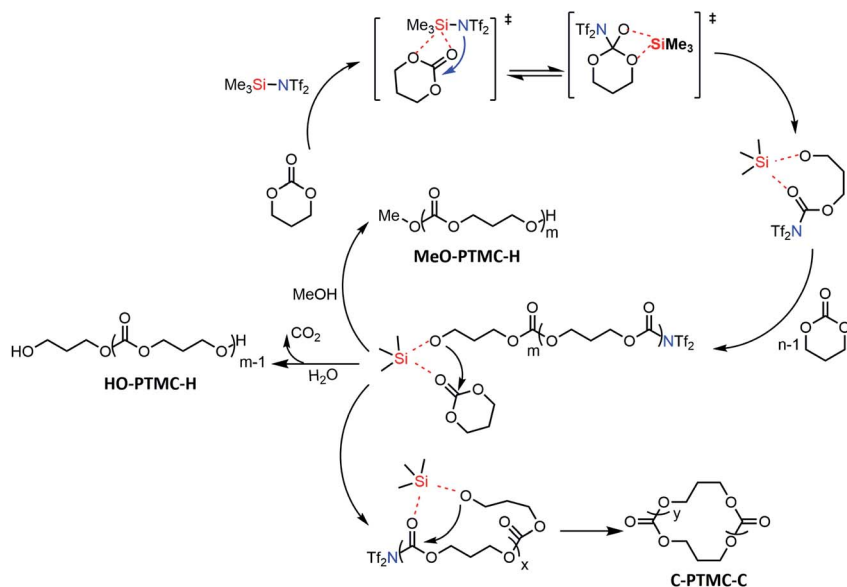


Fig. 4 Chemical shifts of cyclic ester methylene and carbonyl carbon in the  $^{13}\text{C}$  NMR spectra observed by NMR titration of  $\gamma$ -BL with  $\text{TMSNTf}_2$  in  $\text{CDCl}_3$ .



Scheme 3 Proposed plausible metal-free "coordination-insertion" mechanism for the ROP mediated by TMSNTf<sub>2</sub> (TMC as a model monomer).

$-\text{CH}_2\text{CH}_2\text{CH}_2\text{CH}_2\text{CH}_2\text{O-Si}(\text{CH}_3)_3$  was observed at 81.2 ppm, in comparison with the characteristic signal of  $-\text{CH}_2\text{CH}_2\text{CH}_2\text{CH}_2\text{CH}_2\text{OH}$  at 63.8 ppm which was produced by  $\varepsilon\text{-CL/TMSNTf}_2$  in a ratio of 1 : 1 quenched by methanol (Fig. S15a†). Besides, Kricheldorf *et al.* proposed that the ring-opening of lactones and carbonates proceeds through a transition state, in which the carbonyl oxygen is complexed to silicon *via* the vacant orbitals.<sup>10</sup> The above data further confirmed the coordination activation of Si in the TMSNTf<sub>2</sub>-mediated ROP.

## Kinetics

Polymerization kinetics of TMSNTf<sub>2</sub>-mediated ROP of TMC were investigated under standard conditions (see Experimental part), where the initial ratios of monomer to initiator were systematically varied ( $[\text{TMC}]_0 : [\text{TMSNTf}_2]_0 = 20 : 1-100 : 1$ ), while the initial monomer concentration was kept constant ( $[\text{TMC}]_0 = 0.7 \text{ M}$ ). Lines consisting of two linear steps for each case were obtained (Fig. 5A). As shown in Fig. 5B, magnification of the first linear steps of Fig. 5A, the polymerizations exhibit a first-order dependence of the monomer concentration with time (*i.e.*,  $d[\text{M}_1]/dt = k_{\text{obs}}[\text{M}_1]$ ), which is the fingerprint of living polymerization. As the initial TMSNTf<sub>2</sub> concentration increases from 7 to 10, 14 and 32 mM, the observed rate constant ( $k_{\text{obs}}$ ) increases linearly (*i.e.*,  $k_{\text{obs}} = k_p[\text{TMSNTf}_2]_0$ ) from 0.16 to 0.23, 0.32 and 0.71  $\text{h}^{-1}$  (Fig. 5C) giving a  $k_p = 22 \text{ M}^{-1} \text{ h}^{-1}$ . The polymerization kinetics of TMSNTf<sub>2</sub>-mediated ROP of  $\varepsilon\text{-CL}$  were also investigated ( $[\varepsilon\text{-CL}]_0 : [\text{TMSNTf}_2]_0 = 20 : 1-100 : 1$ ,  $[\text{M}]_0 = 1.0 \text{ M}$ ). As shown in Fig. S16A,† all the semilogarithmic plots reveal the same two linear steps with TMC, in which the first step corresponds to a first-order dependence of monomer concentration with time (*i.e.*,  $d[\text{M}_1]/dt = k_{\text{obs}}[\text{M}_1]$ ). The plot of the observed rate constant ( $k_{\text{obs}}$ ) versus the initial TMSNTf<sub>2</sub> concentration of the first step is shown in Fig. S16B,† in which the  $k_{\text{obs}}$  increases from 0.12 to 0.7  $\text{h}^{-1}$  when the initial TMSNTf<sub>2</sub>

concentration increases from 10 to 60 mM. Moreover, the plot of  $k_{\text{obs}}$  versus  $[\text{TMSNTf}_2]_0$  shows a linear relationship (*i.e.*,  $k_{\text{obs}} = k_p[\text{TMSNTf}_2]_0$ ,  $k_p = 11.6 \text{ M}^{-1} \text{ h}^{-1}$ ). All the above data indicate that in the first step of ROP of TMC and  $\varepsilon\text{-CL}$ , TMSNTf<sub>2</sub> acts as a single-site initiator.<sup>19</sup>

After the first step, the plots of  $\ln([\text{TMC}]_0/[\text{TMC}]_t)$  versus reaction time are linear until monomer conversion up to 90%, but with reduced observed rate constants compared to the first step. The fractional dependence with monomer concentration has also been observed for aluminum, yttrium alkoxides, and other systems.<sup>11d,20</sup> According to the previous report, an aggregation process may occur in the second step. The active species of the propagating polymer chain (active silicon group) is stabilized by the excess monomer at the beginning of polymerization, but when the monomer conversion is >50–60%, the concentration of carbonyl group of the monomer decreases a lot accordingly; meanwhile, the carbonyl group of the propagating polymer chain grows a lot. The carbonyl group of polymer will compete with the monomer to occupy the vacant orbitals of the active silicon group at the high monomer conversion, which will reduce the activity of the active silicon group and lead to aggregation of the active silicon group with the polymer chain. The activity loss of the active silicon group results in a slower propagation rate, as shown in Fig. 5A. Similarly, as shown in Fig. S16A,† the aggregation process of TMSNTf<sub>2</sub>-mediated ROP of  $\varepsilon\text{-CL}$  also leads to a slower propagation rate at the high monomer conversion. Therefore, we speculate that the aggregation process is happening in TMSNTf<sub>2</sub>-mediated ROP.

All polymers produced by various initial feeding ratios of monomer to TMSNTf<sub>2</sub> ( $[\text{M}]_0 : [\text{TMSNTf}_2]_0 = 20 : 1-100 : 1$ , Table 1), show monomodal SEC traces (PTMC: Fig. S17; PCL: Fig. S18†). The plots of polymer  $M_n(\text{SEC})$ s as a function of monomer conversion give a linear relationship but somewhat deviate from the theoretical dependencies (TMC, Fig. 5D;  $\varepsilon\text{-CL}$ , Fig. S19†). From the plot of PTMC, the polymer propagating

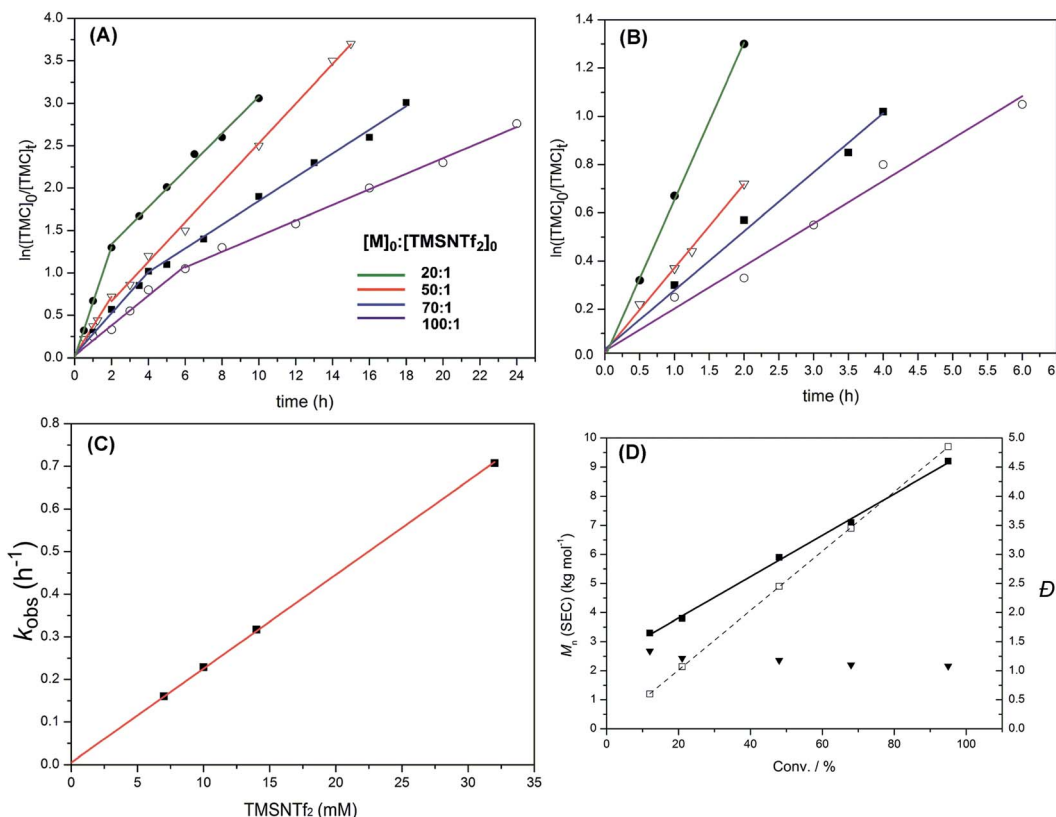


**Fig. 5** (A) Plots of  $\ln([TMC]_0/[TMC]_t)$  versus reaction time for the ROP of TMC initiated by TMSNTf<sub>2</sub> in  $\text{CH}_2\text{Cl}_2$  at various ratios of TMC to TMSNTf<sub>2</sub> ( $[TMC]_0 : [TMSNTf_2]_0 = 20 : 1 - 100 : 1$ ,  $[M]_0 = 0.7 \text{ M}$ ,  $25^\circ\text{C}$ ). (B) Enlargement of the initial linear parts of (A). (C) Plot of the observed rate constant ( $k_{\text{obs}}$ ) versus the initial TMSNTf<sub>2</sub> concentration for the ROP of TMC. (D) Plots of  $M_{n,\text{SEC}}$  versus monomer conversion for the ROP of TMC initiated by TMSNTf<sub>2</sub> (Table 1, entry 5): (■)  $M_n$  (SEC, using the  $dn/dc$  [ $0.0409 \text{ mL g}^{-1}$ ]); (□)  $M_n$  (theory); (▼)  $D$  ( $M_w/M_n$  from SEC).

chains formed in the first step continue growing in the second step. However, the molecular weights of PTMC were higher than the theoretical ones at the beginning and then lower than the theoretical ones. This is due to the weak nucleophilic attack of  $-\text{NTf}_2$  leading to a relatively slower initiation rate as compared to the propagation rate leading to higher molecular weights. Besides, the slower initiation rate than the propagation rate resulted in the broader molecular weight distributions ( $D$ ), as shown in Fig. 5D. When the monomer was consumed, the aggregation of active species to dimeric structure and large clusters occurred, which caused the lower molecular weights. From Fig. S19,† the plot of PCL shows nearly the same phenomenon as PTMC. These results followed the character of a typical metal-complex “coordination-insertion” mechanism in the ROP of cyclic esters for the initiation and propagation steps.

#### TMSNTf<sub>2</sub>-mediated diblock copolymerization of $\varepsilon$ -CL and TMC

Accordingly, we carried out a sequential block copolymerization of  $\varepsilon$ -CL and trimethylene carbonate (TMC) with the initial ratio of  $[\varepsilon\text{-CL}]_0/[TMC]_0/[TMSNTf_2]_0 = 20/30/1$  to produce the well-defined diblock polymer (PCL-*b*-PTMC). The whole process was completed in 22 h, and the chemical structure of the obtained polymer was confirmed by <sup>1</sup>H NMR (Fig. S20†). From the

<sup>1</sup>H NMR spectrum, all the resonance signals could be assigned to the corresponding protons of the main body of PCL-*b*-PTMC. Fig. S21† shows the SEC traces of the PCL homopolymer macroinitiator and the PCL-*b*-PTMC diblock copolymer. After the homopolymerization, the molecular weight ( $M_{n,\text{SEC}}$ ) of polymer increased from  $4.0 \text{ kg mol}^{-1}$  ( $D = 1.25$ ) to  $5.4 \text{ kg mol}^{-1}$  ( $D = 1.19$ ). When the initial ratio of  $[\varepsilon\text{-CL}]_0/[TMC]_0/[TMSNTf_2]_0 = 100/100/1$  was used, the conversion of TMC in the second polymerization was just 51%, even after 100 h. In this case, the molecular weight of the first block is much higher, resulting in reduced propagating reactivity.

## Conclusions

In summary, the first metal-free “coordination-insertion” ring-opening polymerization (ROP) of cyclic carbonate and lactone mediated by TMSNTf<sub>2</sub> was proposed. The metal-free “coordination-insertion” mechanism, monopoly until now of the metal-complexes, is significantly favorable for TMSNTf<sub>2</sub>-mediated ROP of TMC and  $\varepsilon$ -CL, with Si atom acting as a vacant orbitals center (corresponding to the metal) and tertiary amine as an electronegative center (corresponding to the ligand). In the mechanism, the coordination of monomer to Si atom of TMSNTf<sub>2</sub> occurs, followed by a nucleophilic attack on the carbonyl carbon of the coordinated monomer by the  $-\text{NTf}_2$

group, acyl–oxygen cleavage, and insertion of monomer to the Si–N bond of TMSNTf<sub>2</sub>. ROP of TMC and ε-CL mediated by TMSNTf<sub>2</sub> yielded linear and cyclic polymers with two-stage polymerization processes and weak control of molecular weights. In the first stage, the polymerization was initiated by TMSNTf<sub>2</sub> with single-site activation. By detailed NMR studies, including NMR titration experiments and NMR analyses of the intermediate reaction mixture, the metal-free “coordination-insertion” mechanism was proved. In conclusion, we proposed a new initiation/catalytic path of TMSNTf<sub>2</sub> and the concept of a metal-free “coordination-insertion” mechanism, which is unprecedented in the ROP field. Current efforts focus on polymerizations performed with co-initiators and extending variously metal-free coordination-insertion ROPs.

## Data availability

The electronic supplementary information include experimental detail, additional NMR data, SEC data, kinetics data and MALDI-ToF data.

## Author contributions

Zhenjiang Li and Kai Guo conceived the idea and led the project. Xin Wang and Zhenjiang Li designed the experiments. Xin Wang performed the experiments and prepared the ESI.† Xin Wang, Jiaxi Xu, Jingjing Liu, and Zhenjiang Li were involved in the analysis of data. Xin Wang wrote the manuscript. Xin Wang, Zhenjiang Li, Jie Sun, and Nikos Hadjichristidis participated in the discussions and revised the manuscript. All of the authors reviewed, approved, and contributed to the final version of the manuscript.

## Conflicts of interest

There are no conflicts to declare.

## Acknowledgements

This work was supported by the National Natural Science Foundation of China (22078150), the National Key Research and Development Program of China (2017YFC1104802), the Jiangsu National Synergetic Innovation Center for Advanced Materials (SICAM), the project funded by the Priority Academic Program Development of Jiangsu Higher Education Institutions (PAPD), and the Top-Notch Academic Programs Project of Jiangsu Higher Education Institutions (TAPP). N. H. acknowledges the support of King Abdullah University of Science and Technology.

## Notes and references

- 1 W. B. Jensen, *Chem. Rev.*, 1978, **78**, 1–22.
- 2 (a) R. Ligny, M. Hänninen, S. M. Guillaume and J. F. Carpentier, *Angew. Chem., Int. Ed.*, 2017, **56**, 10388–10393; (b) M. Hong and E. Y. X. Chen, *Nat. Chem.*, 2016, **8**, 42–49; (c) E. Martin, P. Dubois and R. Jerome, *Macromolecules*, 2000, **33**, 1530–1535; (d) H. Y. Ma and

- J. Okuda, *Macromolecules*, 2005, **38**, 2665–2673; (e) M. I. Bruce, *Chem. Rev.*, 1998, **98**, 2797–2858.
- 3 (a) K. M. Stridsberg, M. Ryner and A. C. Albertsson, in *Adv Polym Sci*, ed. A. C. Albertsson, Springer-Verlag Berlin, Berlin, 2002, vol. 157, pp. 41–65; (b) L. R. Rieth, D. R. Moore, E. B. Lobkovsky and G. W. Coates, *J. Am. Chem. Soc.*, 2002, **124**, 15239–15248; (c) B. J. O’Keefe, M. A. Hillmyer and W. B. Tolman, *J. Chem. Soc., Dalton Trans.*, 2001, 2215–2224.
- 4 P. P. Power, *Nature*, 2010, **463**, 171–177.
- 5 (a) P. P. Gaspar and R. West, *Silylene chemistry of organic silicon compounds 2, Part 3*, ed. Z. Rappoport and Y. Apeloir, Wiley, 1998, vol. 2, pp. 2463–2568; (b) Y. Mizuhata, T. Sasamori and N. Tokitoh, *Chem. Rev.*, 2009, **109**, 3479–3511; (c) G. Linti and H. Schnockel, *Coord. Chem. Rev.*, 2000, **206**, 285–319.
- 6 (a) D. W. Stephan, *Dalton Trans.*, 2009, 3129–3136; (b) H. Lu and J. J. Cheng, *J. Am. Chem. Soc.*, 2007, **129**, 14114–14115; (c) H. Y. Zhang, Y. Z. Nie, X. M. Zhi, H. F. Du and J. Yang, *Chem. Commun.*, 2017, **53**, 5155–5158.
- 7 (a) Y. Wang, Y. Xie, P. Wei, R. B. King, H. F. Schaefer III, P. v. R. Schleyer and G. H. Robinson, *Science*, 2008, **321**, 1069–1071; (b) Z. D. Wang, J. Y. Zhang, J. F. Li and C. M. Cui, *J. Am. Chem. Soc.*, 2016, **138**, 10421–10424; (c) F. M. Muck, B. Forster, J. A. Baus, M. Nutz, C. Burschka, R. Bertermann and R. Tacke, *Eur. J. Inorg. Chem.*, 2016, **2016**, 3246–3252; (d) G. Frenking, *Angew. Chem., Int. Ed.*, 2014, **53**, 6040–6046; (e) T. W. Bai and J. Ling, *J. Phys. Chem. A*, 2017, **121**, 4588–4593.
- 8 B. Mathieu and L. Ghosez, *Tetrahedron Lett.*, 1997, **38**, 5497–5500.
- 9 H. R. Kricheldorf and J. Jenssen, *J. Macromol. Sci., Part A: Pure Appl. Chem.*, 1989, **26**, 631–644.
- 10 (a) R. Dunsing and H. R. Kricheldorf, *Eur. Polym. J.*, 1988, **24**, 145–150; (b) H. R. Kricheldorf, *Angew. Chem., Int. Ed.*, 1979, **18**, 689–690.
- 11 (a) H. R. Kricheldorf, M. Berl and N. Scharnagl, *Macromolecules*, 1988, **21**, 286–293; (b) P. Dubois, P. Degee, R. Jerome and P. Teyssie, *Macromolecules*, 1992, **25**, 2614–2618; (c) H. R. Kricheldorf, M. V. Sumbel and I. Kreisersanders, *Macromolecules*, 1991, **24**, 1944–1949; (d) P. Dubois, C. Jacobs, R. Jerome and P. Teyssie, *Macromolecules*, 1991, **24**, 2266–2270.
- 12 (a) V. Gutmann, *Electrochim. Acta*, 1976, **21**, 661–670; (b) V. Gutmann, *The donor-acceptor approach to molecular interactions*, Springer, 1978; (c) V. Gutmann, *Pure Appl. Chem.*, 1979, **51**, 2197–2210.
- 13 W. N. Ottou, E. Conde-Mendizabal, A. Pascual, A. L. Wirotius, D. Bourichon, J. Vignolle, F. Robert, Y. Landais, J. M. Sotiropoulos, K. Miqueu and D. Taton, *Macromolecules*, 2017, **50**, 762–774.
- 14 G. Montaudo, M. S. Montaudo, C. Puglisi, F. Samperi, N. Spassky, A. LeBorgne and M. Wisniewski, *Macromolecules*, 1996, **29**, 6461–6465.
- 15 M. H. Chisholm and E. E. Delbridge, *New J. Chem.*, 2003, **27**, 1177–1183.



16 S. Antoniotti, V. Dalla and E. Dunach, *Angew. Chem., Int. Ed.*, 2010, **49**, 7860–7888.

17 N. Spassky, V. Simic, M. S. Montaudo and L. G. Hubert-Pfalzgraf, *Macromol. Chem. Phys.*, 2000, **201**, 2432–2440.

18 (a) A. Kowalski, J. Libiszowski, A. Duda and S. Penczek, *Macromolecules*, 2000, **33**, 1964–1971; (b) Y. Takashima, Y. Nakayama, K. Watanabe, T. Itono, N. Ueyama, A. Nakamura, H. Yasuda, A. Harada and J. Okuda, *Macromolecules*, 2002, **35**, 7538–7544; (c) M. Save and A. Soum, *Macromol. Chem. Phys.*, 2002, **203**, 2591–2603.

19 B. J. O'Keefe, L. E. Breyfogle, M. A. Hillmyer and W. B. Tolman, *J. Am. Chem. Soc.*, 2002, **124**, 4384–4393.

20 (a) M. Cheng, D. R. Moore, J. J. Reczek, B. M. Chamberlain, E. B. Lobkovsky and G. W. Coates, *J. Am. Chem. Soc.*, 2001, **123**, 8738–8749; (b) C. X. Cai, A. Amgoune, C. W. Lehmann and J. F. Carpentier, *Chem. Commun.*, 2004, 330–331; (c) A. Duda and S. Penczek, *Macromol. Rapid Commun.*, 1994, **15**, 559–566.

